Structural and Optical Studies of Ni/S Co Doped TiO_2 Nanorods via Sol-Gel Route

V. Kavitha, P.S. Ramesh and D. Geetha

Abstract Nano crystalline TiO_2 particles doped with various concentrations of Ni/S were successfully synthesized via sol-gel route using titanium tetra isopropoxide while titanium precursor, Ni $(NO_3)_2.6H_2O$ (nickel source) and CS $(NH_2)_2$ (sulfur source). The prepared particles were characterized by standard analytical techniques such as X-ray diffraction (XRD), Fourier transform infrared spectroscopy (FT-IR), UV-Vis absorption spectroscopy, scanning electron microscopy/energy dispersive spectroscopy (SEM/EDS), and transmission electron microscopy (TEM). The photocatalytic activity of Ni/S-TiO_2 is estimated through photocatalytic degradation of Rhodamine B solution under UV irradiation. The XRD data exhibit that the average crystallite size decreases with increase in Ni/S proportions in TiO_2 and the crystal structure of TiO_2 does not change upon the loading of Ni/S. The particles shape changes from spherical to rod and hence rod-like particles are dominant and lightly stuck together. The spectra of pure TiO_2 and doped TiO_2 explains emission peak is a blue shift and seen that maximum peak is around 410 nm. This maximum peak shift mainly aspect to increased electron density at oxygen site. In PL spectra emissions observed for all the doped samples are attributed to the oxygen vacancies and Ti vacancies introduced after Ni/S doping. Compared with pure TiO_2 nanoparticles, Ni/S doped TiO_2 photocatalyst exhibited high photocatalytic activity under ultraviolet (UV) irradiation in the degradation of Rhodamine B aqueous solution. The maximum 97 % of degradation efficiency of Rhodamine B was observed at 3:1 Ni/S-TiO_2 within 120 min. The photocatalytic efficiency of Rhodamine B of Ni/S doped TiO_2 nanoparticle was higher than that of pure TiO_2.

V. Kavitha
Department of Physics, Periyar University, 636011 Salem, Tamil Nadu, India

P.S. Ramesh (✉)
Department of Physics, Wing DDE, Annamalai University, 608002 Chidambaram, Tamil Nadu, India
e-mail: psrddephyau@gmail.com

D. Geetha
Department of Physics, Annamalai University, 608002 Chidambaram, Tamil Nadu, India

J. Ebenezar (ed.), *Recent Trends in Materials Science and Applications*,
Springer Proceedings in Physics 189, DOI 10.1007/978-3-319-44890-9_28

1 Introduction

In recent years, the titanium dioxide (TiO_2) nanostructures have fascinated significant interest because of their unique properties and many potential applications in various fields such as catalysis [1, 2], photo-catalysis [3, 4], sensors [5, 6], solar cells [7, 8], energy storage [9], and gene therapy [10]. It has been established that the physical and chemical properties of TiO_2 nanostructure and great potential applications based on their particle size, crystalline structure and morphology [11].

In the present scenario, photocatalysis has attracting intensive interest owing to its promising applications particularly in environmental remediation and clean energy production. TiO_2 powder is most attractive semiconductors for a photocatalyst and broadly applied in diverse fields, such as decomposition of organic contaminants, water and gas streams treatment, and water photo splitting into H_2 and O_2 [12–14]. Generally, the photocatalytic activity of the TiO_2 depends on more than a few factors such as crystal size, phase and surface area and also depends upon additional factors one is separation efficiency of electron-hole pair, recombination rate of photogenerated electron and hole pairs [15–17].

Doping with metal and non-metal ions is a popular method which facilitates UV light activity of TiO_2. Many investigations have been conducted to extend optical absorption of TiO_2 based materials to the visible light region and to improve photocatalytic activity by nonmetal doping using N [18], C [19, 20], S [21] or multi elemental doped materials [22, 23]. The doping of different transitional metal ions into TiO_2 could shift its optical absorption edge from UV to visible light range, but a prominent change in TiO_2 band gap was not observed [24]. However, transition metal ion-doped TiO_2 suffers from some serious disadvantages, such as thermal instability and low quantum efficiency of the photoinduced charge carriers (electron—hole pairs) [25]. In order to further develop the photocatalytic activity, co-doped titania with double non-metal [26–28], metal–non-metal [29–31] and metal–metal ion [32] has attracted more attention. Most of these explorations have been demonstrated under UV light, because titanium dioxide exhibit relatively high photocatalytic activity and chemical stability under UV light.

In particular, TiO_2 photocatalysts co-doped with S and another metal had attracted many attentions in recent years. For example, prepared Ag and S doped TiO_2 photocatalysts by a photo induced deposition method with high photocatalytic activity for the degradation of Congo red both under UV light, solar light irradiation [33]. The Cu and S co-doped TiO_2 photocatalysts by a sol-gel method with degradation of methyl orange [34].

The aim of the present work is to prepare TiO_2 particles co-doped with Nickel and Sulfur (Ni/S-TiO_2) via sol-gel route, to develop the photocatalytic performance using Rhodamine B. In comparison with other synthesis methods, sol-gel process has notable advantages such as high purity and low temperature, etc.

2 Experimental

2.1 Materials

All of the chemical reagents of analytical grade and were used as without any further purification. Titanium (IV) isopropoxide, ($C_{12}H_{28}O_4Ti$, purity 97 % Sigma Aldrich) was used as starting to prepare crystalline TiO_2 nanoparticles. Ni $(NO_3)_2{\cdot}6H_2O$, CS $(NH_2)_2$ and nitric acid were dopant precursor obtained from Hi-media. Rhodamine B was purchased from sigma-Aldrich. De-ionized water is used for to prepare TiO_2 nanoparticles.

2.2 Synthesis

TiO_2 nanoparticles were synthesized via sol-gel route, involving hydrolysis and condensation of Titanium tetra isopropoxide (TTIP). The 5 ml of TTIP was dissolved in 20 ml of isopropanol. This chemical solution drop wise added into the de-ionized water maintained at pH (2–4) using HNO_3. The solution was well stirred for 30 min, to get clear solution. The dopant precursors Ni $(NO_3)_2.6H_2O$ and CS $(NH_2)_2$ are dissolved in de-ionized water and added into the above solution. The solution of both Ni/S and Ti were stirred for 8 h until a transparent gel is formed. After a period, the gel was dried at 100 °C and washed with ethanol several times, grinded into fine sample powder and then calcined at 500 °C for 4 h. This route was adopted as an optimized method for the preparation of TiO_2 nanoparticles.

2.3 Characterization

The X-ray diffraction patterns of the synthesized samples were recorded on a XPERT-PRO X-ray diffractometer with Cu-Kα radiation (λ = 0.15418 nm) and the 2θ range from 20° to 70°. UV-Visible spectra were recorded using UV-1650 shimadzu spectrophotometer. The photoluminescence (PL) spectra of the sample were characterized on a VARIAN photoluminescence. Fourier transform infrared (FT-IR) spectroscopy test was recorded with AVATAR 330 FT-IR spectrometer in the ranging from 4000 to 400 cm^{-1}. SEM image was taken using JEOL, Model JSM 6390. SEM/EDS analysis was carried out on a Scanning Electron Microscope (JEOL-JSM—5610 LV with INCA with EDS. Transmission electron microscope (TEM) analysis were carried out using a JEOL JEM—2011.

2.4 Photocatalytic Activity

The photocatalytic activity of pure TiO_2 nanoparticles and doping samples were investigated by measuring the photodegradation of Rhodamine B in aqueous solution under UV light irradiation. After the visible light irradiation, the color solution changes from initial pink-red to colorless, revealing that the chromophoric structure of the Rhodamine B is destroyed with the photoreaction time.

3 Results and Discussion

3.1 X-ray Diffraction Studies

Figure 1 shows XRD diffraction patterns of (Ni/S) co-doped TiO_2 nanoparticles synthesized via sol-gel route. The diffraction pattern of TiO_2 is good agreement with JCPDS card No 21-1272 for TiO_2. The peak positions obtained at 25.61, 37.61, 38.58, 48.21, 53.98, 55.06, 62.74, 68.88, and 70.28 are typical patterns of anatase, corresponding crystal planes are (101), (004), (112),(200), (105), (211), (204), (116), and (220) respectively. It can also be seen from Fig. 1 Ni/S-TiO_2 are present in anatase phase, while the adding of Ni does not influence the crystallization performance of TiO_2. In addition, the reflection peak of Ni in Ni/S-TiO_2 is

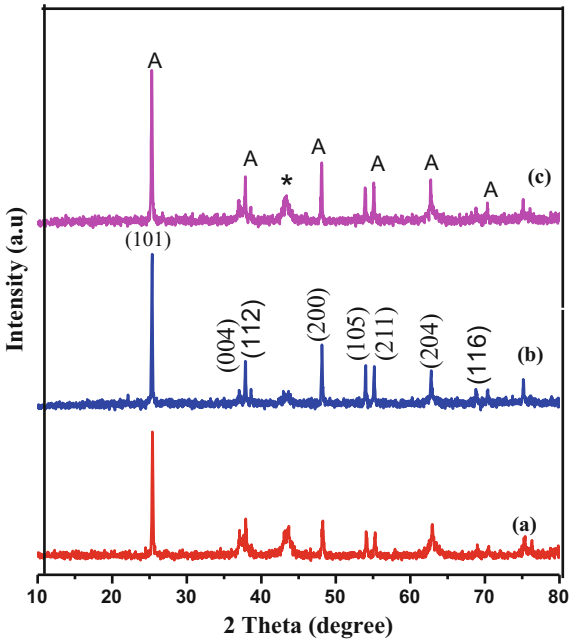

Fig. 1 X-ray diffraction of Ni/S co-doped TiO_2 **a** (1:1) Ni/S **b** (2:1) Ni/S, **c** (3:1) Ni/S *A* and *asterisk* indicates anatase and Ni

presents at 2θ = 44.01°, which is indicated with an asterisk and it well accords with JCPDS No: 04-0850 for Ni with face centered cubic (FCC) crystalline structure. The reflection peak corresponds to the Ni (111) crystal plane, revealing that Ni has been successfully loaded on TiO_2 [35]. The average particle size was estimated using the Scherrer's equation:

$$D = 0.89\lambda/\beta \cos\theta$$

where λ is the wavelength of the Cu Kα radiation, β is the full width at half maximum (FWHM) of the diffraction peak and θ is the Bragg angle. The average crystallite size was found to be 40 nm, 37 nm, and 36 nm for Ni/S-TiO_2 (1:1), Ni/S-TiO_2 (2:1) and Ni/S-TiO_2 (3:1), respectively.

3.2 *Functional Group Analysis (FT-IR)*

The infrared spectroscopy of pure TiO_2 and Ni/S-doped TiO_2 is represented in Fig. 2. The absorption band at 1626.3 cm^{-1} is attributed to the stretching vibration of O–H groups in absorption water [36]. The strong peaks corresponding to 1131 cm^{-1} are the characteristic frequencies of SO_4^{2-} with bidentate bond [37, 38]. Therefore, the most possible doping process is the SO_4^{2-} incorporated into the network of Ti–O–Ti. The presence of sulfate might be responsible for the formation of anatase nucleus and preventing the growth of crystalline size. Some weak bands

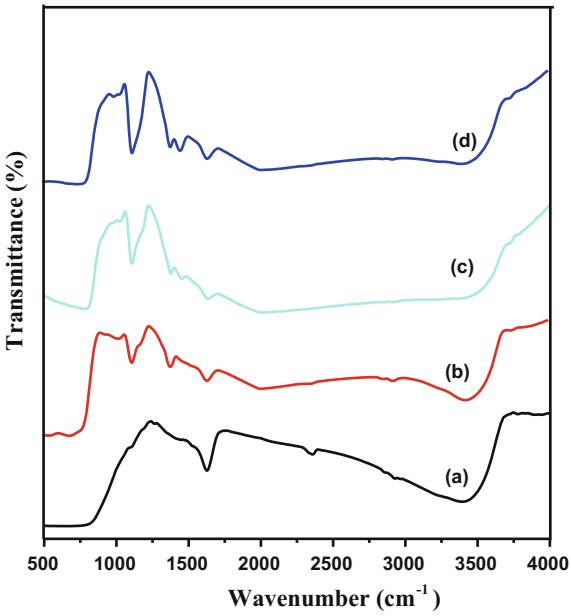

Fig. 2 FT-IR spectra of **a** Pure TiO_2 **b** (1:1) Ni/S **c** (2:1) Ni/S **d** (3:1) Ni/S

between 3400 and at 1630 cm^{-1} are seen, which decreased due to the existence of Ni/S over TiO_2 surface [39, 40]. These bands are attributed to the stretching vibration modes of the O–H groups and the bending modes of the absorbed water molecules, respectively. Further, the broad intense band seen below 900 cm^{-1} is due to Ti–O–Ti vibrations. This shifts to the lower wave numbers and is sharpening which can be attributed to increase in the size of TiO_2 particles after nickel reduction. These results imply additional transmittance bands in Ni/S-doped TiO_2, in comparison to pure TiO_2 powders [39].

3.3 Surface Morphological Analysis

3.3.1 Scanning Electron Microscopy (SEM/EDS)

SEM is one of the powerful tools to analyze surface morphology of the sample and it provides information regarding the growth mechanism, size and shape of the nanoparticles. The surface morphology of the TiO_2 nanoparticles is shown in Fig. 3a–c. The shape of the particles changes from spherical to rod and hence rod-like nanoparticles are dominant and lightly stuck together, with particle size around
35–45 nm.

Energy dispersive X-ray spectrometer (EDS) is an efficient analytical technique used for the elemental composition analysis of a product. The EDS of the TiO_2 nanomaterials are shown in Fig. 4. The EDS result demonstrates the phase of titanium (Ti), Nickel (Ni) and oxygen (O) and sulfur (S) are present in the sample.

3.3.2 Transmission Electron Microscopy (TEM)

Figure 5 presents TEM micrographs of Ni/S-doped (3:1) TiO_2 photocatalysts obtained by the sol-gel method. It can be seen that there were many rod like nanoparticles. It showed good agreement with the result of SEM.

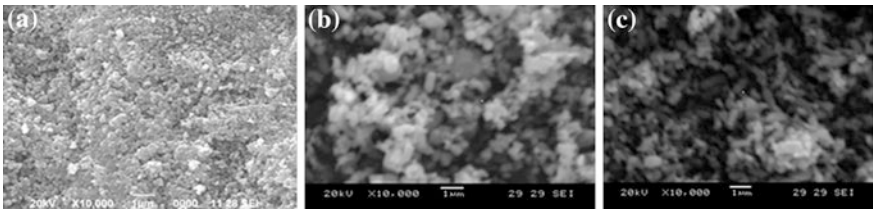

Fig. 3 SEM image of **a** (1:1) Ni/S **b** (2:1) Ni/S **c** (3:1) Ni/S

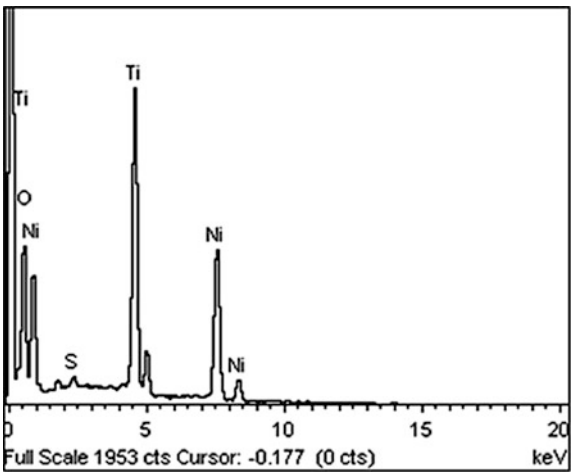

Fig. 4 EDS spectrum of (3:1) Ni/S doped TiO_2

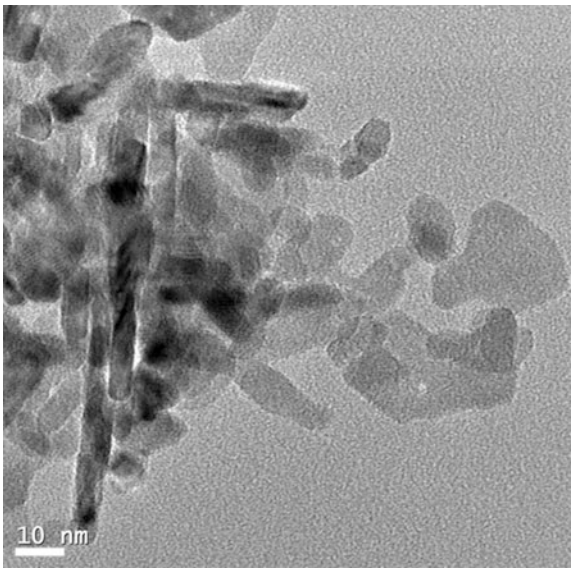

Fig. 5 TEM micrograph of (3:1) Ni/S-TiO_2

3.4 Optical Absorption Analysis (UV-Vis Spectroscopy)

The UV-Vis absorbance spectra of pure TiO_2 and Ni/S doped TiO_2 samples are shown in Fig. 6. The absorption of Ni/S-TiO_2 was located at 300 nm in the UV region. Upon increasing the Ni/S content, the intensity of absorption peak rapidly increased. The longer wavelength absorption can be assigned to the formation of impurity levels within the band gap energy of titanium dioxide. The absorption

wavelength is greater than 400 nm it will affect the formation of electron-hole pairs and separation in a photocatalytic application in the visible region [41, 42].

The band gap energy (eV) of the nanomaterials was quantified using Tauc equation. The E_{bg} estimated from the intercept of tangents to the plots is 3.82 eV for TiO_2, 3.2, 3.1, 2.8 eV for Ni/S doped TiO_2.

3.5 Photoluminescence Studies (PL)

The photoluminescence spectra of all prepared powder samples exhibit broad peaks in the wavelength ranging from 350 to 530 nm with the excited wavelength of 290 nm in Fig. 7. The spectra of Ni/S-TiO_2 and TiO_2 are similar and demonstrate the peak approximately 410 nm. When compared with the band gap energy of TiO_2 (3.2 eV), the broad asymmetric peak seen around 410 nm demonstrates that the emission does not arise. Previous works have proposed that the photoluminescence signals obtained from TiO_2 are generally originating from the surface states resulting from the defects present on the surface of TiO_2 sample [43, 44]. A comparison of the photoluminescence spectra of pure TiO_2 and doped TiO_2 samples with the reported ones shows that the PL signals are largely arising from the levels induced by the defects present in them. The PL spectra of pure TiO_2 and doped TiO_2 show emission peak is blue shift and peak maximum is around 410 nm.

3.6 Photocatalytic Evaluation

Irradiation of UV rays on an aqueous solution of Rhodamine B in the synthesized samples leads to decrease in absorption intensity. The degradation of the

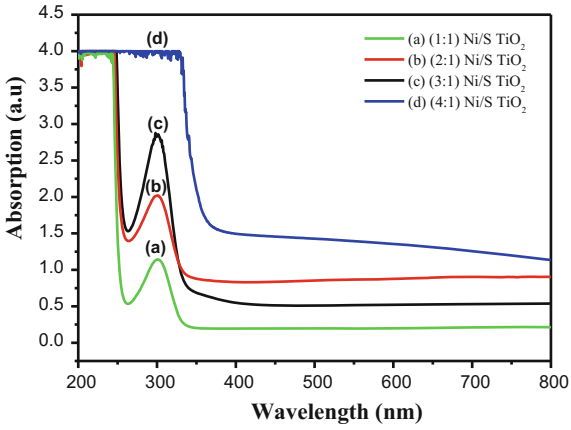

Fig. 6 UV-Visible spectra of **a** (1:1) Ni/S **b** (2:2) Ni/S **c** (3:3) Ni/S **d** Pure TiO_2

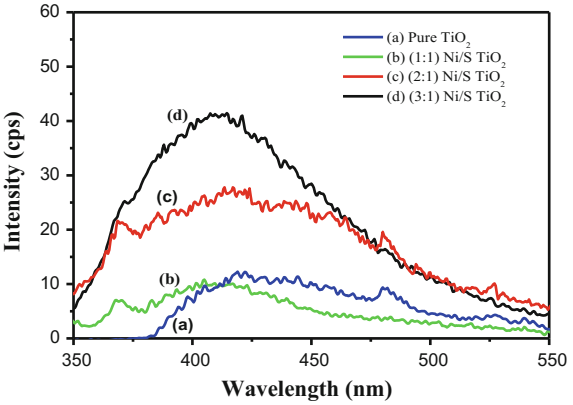

Fig. 7 PL spectra of **a** pure TiO_2 **b** (1:1) Ni/S **c** (2:2) Ni/S **d** (3:3) Ni/S

Rhodamine B under UV light irradiation was determined using a UV-Vis spectrophotometer. The result obtained during the illumination of the Ni/S doped TiO_2 photocatalysts with UV light are revealed in Figs. 8, 9. The photocatalytic response of TiO_2 and Ni/S-TiO_2 was evaluated by monitoring the photo degradation of Rhodamine B in aqueous solution. Typically 25 mg (2.5×10^{-4}) of Rhodamine B dye was added to 250 ml of distilled water used as stocked solution. Prior to the experiment, a suspension was prepared by adding 50 mg of catalyst to 50 ml of Rhodamine B solution. The mixed solution was irradiated using mercury vapor lamp (λ_{max} = 365 nm) under stirring. Further samples were taken out every 30 min and the photocatalyst was separated from the mixture solution and then the UV–Vis absorption of the clarified solution was investigated with a UV–Vis spectrometer. The absorbance of Rhodamine B solution was determined at a wavelength of 465 nm, which corresponds to the maximum absorption wavelength of Rhodamine B.

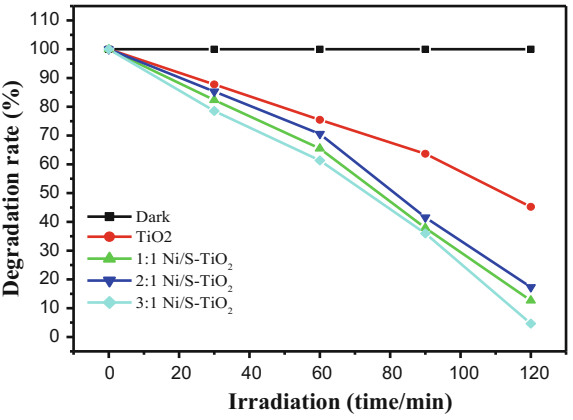

Fig. 8 Typical plot for comparison of change in concentration versus irradiation time in presence of pure TiO_2 and various % of Ni/S doped TiO_2

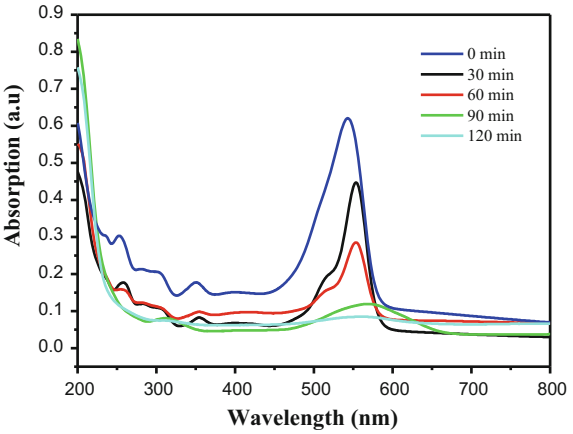

Fig. 9 UV-Visible absorption spectra of Rhodamine B photo degradation under UV light using (3:1) Ni/S doped TiO_2

Figure 8 shows the change in concentration as a function of irradiation time for the dye derivative in the absence and presence of pure and different percentage of Ni/S-doped TiO_2. It is evident that under UV irradiation, no observable loss of Rhodamine B takes place if the reaction was performed in the absence of photocatalysts which exhibits that Rhodamine B is stable under UV irradiation. They reveal that the photocatalytic activities and photodegradation rates increase with increase of Ni/S-TiO_2 nanoparticles. In addition, the Ni/S-doped TiO_2 nanoparticles are more photoactive than the pure TiO_2. It has been found that irradiation of aqueous suspension of Rhodamine B in the presence of prepared photocatalyst illustrates favorable result and leads to decrease in absorption intensity.

The UV-Visible absorption spectra of Rhodamine B degradation are shown in Fig. 9. It decreases in the absorption band of Rhodamine B in the visible state during the irradiation of 120 min. It is found that the maximum absorbance at 553 nm gradually decreases with passage of time and disappears almost completely after 120 min, which indicates the Rhodamine B dye in the presence of synthesized 3:1 Ni/S-doped TiO_2 under UV-light irradiation.

4 Conclusion

The Ni doped titania nanorods were synthesized by sol-gel method and calcinated at 500 °C. The synthesized materials were systematically characterized by XRD, SEM, TEM, UV-Vis, PL and photoconductivity measurements. The Ni/S-doped TiO_2 nanorods are anatase in phase with no other additional impurity phase in the samples. The XRD result indicates that the average crystallite size decreases with increase in Ni concentrations in TiO_2 which is consistent with the morphology observed by SEM and TEM images. The shape of the particles changes from spherical to rod and hence rod-like particles are dominant and lightly stuck together,

with particle size around 35–45 nm. The spectra of pure TiO_2 and Ni/S doped TiO_2 show a blue shift of the emission peak and the peak maximum is seen around 410 nm. The observed trap depth value is greater in the samples than the previously published results on TiO_2 nanoparticles. The present work suggest that semiconducting oxide materials can have promising potential applications in optoelectronic devices such as solar cells, photoconductors in replacement of expansive materials by fine controlling of the compositions and morphology in the oxide materials.

References

1. Yang, G., Yan, Z., Xiao, T., Yang, B.: Low-temperature synthesis of alkalis doped TiO_2 photocatalysts and their photocatalytic performance for degradation of methyl orange. J. Alloys Comp. **580**, 15–22 (2013)
2. De la Cruz, N., Dantas, R.F., Gimenez, J., Esplugas, S.: Photolysis and TiO_2 photocatalysis of the pharmaceutical propranolol: Solar and artificial light. Appl. Catal. B: Environ. **130–131**, 249–256 (2013)
3. Fittipaldi, M., Gatteschi, D., Fornasiero, P.: The power of EPR techniques in revealing active sites in heterogeneous photocatalysis: the case of anion doped TiO_2. Catal. Today **206**, 2–11 (2013)
4. Kamegawa, T., Sonoda, J., Sugimura, K., Mori, K., Yamashita, H.: Degradation of isobutanol diluted in water over visible light sensitive vanadium doped TiO_2 photocatalyst. J. Alloys Comp. **486**, 685–688 (2009)
5. Moon, H.G., Jang, H.W., Kim, J.S., Park, H.H., Yoon, S.J.: A route to high sensitivity and rapid response Nb_2O_5-based gas sensors: TiO_2 doping, surface embossing, and voltage optimization. Sens. Actuat. B **153**, 37–43 (2011)
6. Lee, J., Kim, D.H., Hong, S.H., Jho, J.Y.: A hydrogen gas sensor employing vertically aligned TiO_2 nanotube arrays prepared by template-assisted method Sens. Actuat. B **160**, 1494–1498 (2011)
7. Gratzel, M.: Photoelectrochemical cells. Nature **414**, 338–344 (2001)
8. Shalan, A.E., Rashad, M.M., Yu, Y., Lira-Cantu, M., Abdel-Mottaleb, M.S.A.: Controlling the microstructure and properties of titania nanopowders for high efficiency dye sensitized solar cells Electrochim. Acta **89**, 469–478 (2013)
9. Kim, J.H., Zhu, K., Kim, J.Y., Frank, A.J.: Tailoring oriented TiO_2 nanotube morphology for improved Li storage kinetics Electrochim. Acta **88**, 123–128 (2013)
10. Dhandapani, P., Maruthamuthu, S., Rajagopal, G.: Bio-mediated synthesis of TiO_2 nanoparticles and its photocatalytic effect on aquatic biofilm. J. Photochem. Photobiol. B: Biol. **110**, 43–49 (2012)
11. Song, K., Han, X., Shao, G.: Electronic properties of rutile TiO_2 doped with 4*d* transition metals: First-principles study. J. Alloys Comp. **551**, 118–124 (2013)
12. Fujishima, A., Zhang, X.T.: Titanium dioxide photocatalysis: present situationand future approaches. C. R. Chim. **9**, 750–760 (2006)
13. Hoffmann, M.R., Martin, S.T., Choi, W., Detlef, W.B.: Environmental applications of semiconductor photocatalysis. Chem. Rev. **95**, 69–96 (1995)
14. Zaleska. A.: Doped-TiO_2. A review, Recent Patents Eng. **2**, 157–164 (2008)
15. Kavan, L., Gratzel, M., Gilbert, S.E., Klemenz, C., Scheel, H.J.: Electrochemical and photoelectrochemical investigation of single crystal anatase. J. Am. Chem. Soc. **118**, 6716–6723 (1996)
16. Li, W., Zeng, T.: Preparation of TiO_2 anatase nanocrystals by $TiCl_4$ hydrolysis with additive H_2SO_4. PLoS ONE **6**, e21082 (2011)

17. Mir, N., Salavati-Niasari, M.: Photovoltaic properties of corresponding dye sensitized solar cells: effect of active sites of growth controller on TiO_2 nanostructures. Sol. Energy **86**, 3397–3404 (2012)
18. Yu, J.C., Ho, W.K., Yu, J.G., Yip, H.Y., Wong, P.K., Zhao, J.C.: Efficient visible-light induced photocatalytic disinfection on sulfur-doped nanocrystalline titania. Environ. Sci. Technol. **39**, 1175–1179 (2005)
19. Ho, W.K., Yu, J.C., Lee, S.C.: Synthesis of hierarchical nanoporous F-doped TiO_2 spheres with visible light photocatalytic activity. Chem. Commun. **10**, 1115–1117 (2006)
20. Sun, H.Q., Wang, S., Ang, H.M., Tadé, M.O., Li, Q.: Halogen element modified titanium dioxide for visible light photocatalysis. Chem. Eng. J. **162**, 437–447 (2010)
21. Liu, G., Chen, Z.G., Dong, C.L., Zhao, Y.N., Li, F., Lu, G.Q., Cheng, H.M.: Visible light photocatalyst: iodine-doped mesoporous titania with a bicrystalline framework. J. Phys. Chem. B **110**, 20823–20828 (2006)
22. Hong, X.T., Wang, Z.P., Cai, W.M., Lu, F., Zhang, J., Yang, Y.Z., Ma, N., Liu, Y.J.: Visiblelight- activated nanoparticle photocatalyst of iodine-doped titanium dioxide. Chem. Mater. **17**, 1548–1552 (2005)
23. Usseglio, S., Damin, A., Scarano, D., Bordiga, S., Zecchina, A., Lamberti, C.: (I2)n encapsulation inside TiO_2: a way to tune photoactivity in the visible region. J. Am. Chem. Soc. **129**, 2822–2828 (2007)
24. Wu, J.C.S., Chen, C.H.: A visible-light response vanadium-doped titania nanocatalyst by sol–gel method. J. Photochem. Photobiol. A: Chem. **163**, 509–515 (2004)
25. Choi, W., Termin, A., Hoffmann, M.R.: The role of metal ion dopants in quantum-sized TiO_2: correlation between photoreactivity and charge carrier recombination dynamics. J. Phys. Chem. B **98**(51), 13669–13679 (1994)
26. Ohno, T., Tsubota, T., Nakamura, Y., Sayama, K.: Preparation of S, C cation-codoped $SrTiO_3$ and its photocatalytic activity under visible light. Appl. Catal. A: Gen. **288**, 74–79 (2005)
27. Lin, L., Zheng, R.Y., Xie, J.L., Zhu, Y.X., Xie, Y.C.: Synthesis and characterization of phosphor and nitrogen co-doped titania. Appl. Catal. B: Environ. **76**, 196–202 (2007)
28. Li, X., Xiong, R., Wei, G.: S-N Co-doped TiO_2 photocatalysts with visible-light activity prepared by sol-gel method. Catal. Lett. **125**, 104–109 (2008)
29. Hamal, D.B., Klabunde, K.J.: Synthesis, characterization, and visible light activity of new nanoparticle photocatalysts based on silver, carbon, and sulfur-doped TiO_2. J. Colloid Interf. Sci. **311**, 514–522 (2007)
30. Obata, K., Irie, H.K.: Enhanced photocatalytic activities of Ta, N co-doped TiO_2 thin films under visible light Chem. Phys. **339**, 124–132 (2007)
31. Pingxiao, W., Jianwen, T., Zhi, D.: Preparation and photocatalysis of TiO_2 nanoparticles doped with nitrogen and cadmium. Mater. Chem. Phys. **103**, 264–269 (2007)
32. Zhang, D.R., Kim, Y.H., Kang, Y.S.: Preparation and photocatalysis of TiO_2 nanoparticles doped with nitrogen and cadmium. J. Curr. Appl. Phys. **6**, 801–804 (2006)
33. Gomathi Devi, L., Kavitha, B., Nagaraj.: Bulk and surface modification of TiO_2 with sulphur and silver: Synergetic effects of dual surface modification in the enhancement of photocatalytic activity. Mater. Sci. Semicond. Process. 40832–8392 (2015)
34. Hamadanian, M., Reisi-Vanani, A., Majedi, A.: A.: Synthesis, characterization and effect of calcination temperature on phase transformation and photocatalytic activity of Cu, S-codoped TiO_2 nanoparticles. Appl. Surf. Sci. **256**, 1837–1844 (2010)
35. Liu, Yanhua, Wang, Zilong, Fan, Weibo, Geng, Zhongrong, Fengn, Libang: Enhancement of the photocatalytic performance of Ni-loaded TiO_2 photocatalyst under sunlight. Ceram. Int. **40**, 3887–3893 (2014)
36. Xu, G.Q., Zheng, Z.X., Wu, Y.C.: Feng. N. Effect of silica on the microstructure and photocatalytic properties of titania. Ceram. Int. **35**, 1–5 (2009)
37. Sivakumar, S., Pillai, P.K., Mukundan, P., Warrier, K.G.K.: Sol–gel synthesis of nanosized anatase from titanyl sulfate. Mater. Lett. **57**, 330–335 (2002)

38. Parida, K.M., Sahu, N., Biswal, N.R., Naik, B., Pradhan, A.C.: Preparation, characterization, and photocatalytic activity of sulfate-modified titania for degradation of methyl orange under visible light. J. Colloid Interface Sci. **318**, 231–237 (2008)
39. Ibram Ganesh, A.K., Gupta, P.P., Kumar, P.S.C., Sekhar, K., Radha, G., Sundararajan, G.: Preparation and characterization of Ni-Doped TiO_2 materials for photocurrent and photocatalytic applications. Sci. World J. 1–16 (2012)
40. Begum, N.S., Ahmed, H.M.F., Gunashekar, K.R.: Effects of Ni doping on photocatalytic activity of TiO_2 thin films prepared by liquid phase deposition technique. Bull. Mater. Sci. **31**, 747–751 (2008)
41. Zeng, P., Zhang, X., Zhang, X., Chai, B., Peng, T.: Efficient photocatalytic hydrogen production over Ni@C/TiO_2 nanocomposite under visible light irradiation. Chem. Phys. Lett. **503**, 262–265 (2011)
42. Dai, K., Peng, T.Y., Ke, D.N., Wei, B.Q.: Photocatalytic hydrogen generation using a nanocomposite of multi-walled carbon nanotubes and TiO_2 nanoparticles under visible light irradiation. Nanotechnology **20**, 125603 (2009)
43. Sasikala, R., Sudarsan, V., Sudakar, C., Naik, R., Panicker, L., Bharadwaj, S.R.: Modification of the photocatalytic properties of self doped TiO_2 nanoparticles for hydrogen generation using sunlight type radiation. Int. J. Hydrogen Energy **34**, 6105–6113 (2009)
44. Madhukumar, P., Badrinarayan, S., Sastry, M.: Nanocrystalline TiO_2 studied by optical, FTIR and X-ray photoelectron spectroscopy: correlation to presence of surface states. Thin Solid Films **358**, 122–130 (2000)